
LiB₃O₅ pyroceramic for thermoluminescent dosimeters

¹ Adamiv V. T., ¹ Burak Ya. V., ¹ Teslyuk I. M., ² Antonyak O. T.,
³ Moroz I. E. and ^{4,5} Malynych S. Z.

¹ Vlokh Institute of Physical Optics, 23 Dragomanov Street, 79005 Lviv, Ukraine

² Department of Experimental Physics, Ivan Franko Lviv National University,
8 Kyrilo and Methodiy Street, 79005 Lviv, Ukraine

³ Department of Physics, Lviv Polytechnic National University, 12 S. Bandera
Street, 79013 Lviv, Ukraine

⁴ Department of Photonics, Lviv Polytechnic National University, 12 S. Bandera
Street, 79013 Lviv, Ukraine

⁵ Department of Electromechanics and Electronics, Hetman Petro Sahaidachnyi
National Army Academy, 32 Heroes of Maidan Street, 79012 Lviv, Ukraine

Received: 23.09.2019

Abstract. We report on preparation procedures and thermoluminescent properties of undoped and Ag-doped lithium triborate (LiB₃O₅) pyroceramics. They are prepared using a technique of special annealing of LiB₃O₅ glass. X-ray diffraction studies of our pyroceramic reveal formation of a large number of nanosized crystallites within amorphous matrix. The crystalline structure and the nature of thermoluminescence in the LiB₃O₅ pyroceramic are discussed. We demonstrate that this pyroceramic represents a material promising for radiation dosimetry.

Keywords: lithium triborate, glasses, pyroceramic, thermoluminescence, radiation dosimeters

UDC: 535.37

1. Introduction

In the recent decades, a great number of studies have been devoted to the materials possessing thermoluminescence (TL), which can be exploited in radiation dosimetry. Borate compounds are promising for TL dosimetry since they are chemically stable and, moreover, they exhibit high sensitivity and bright above-room-temperature TL peaks [1–3]. The first studies of TL properties of the lithium-borate compounds have been performed by Schulman et al. as early as in 1967 [4]. Among the borates, lithium triborate LiB₃O₅ (abbreviated hereafter as LBO) is especially suitable for the TL dosimetry, since it has the equivalent absorption coefficient $Z_{eff} = 7.3$, which is close to that of human tissue. This material is widely used in radiation therapy. In addition, doped LBO has a potential as a new material for neutron detection, due to a presence of ⁶Li and ¹⁰B isotopes exhibiting high neutron-capture cross-sections. Issuing from the phase diagram of Li₂O–B₂O₃ compounds considered in detail in Ref. [5], the process of LBO melting at the temperature ~ 834°C has incongruent character. Hence, a solid-state reaction technique should be used in order to synthesize LBO at the temperatures below 834°C [6–9].

Undoped LBO does not have a sufficient TL dose response [10]. However, its TL properties can be improved substantially upon sensitizing [11–13]. Depci et al. [14] have reported on the TL properties of LBO doped with rare-earth elements (Y and Ce–Lu). The influence of such dopants as CuO, MnO₂, Fe₂O₃, CoCO₃, MgO and Al₂O₃ on the TL properties of LBO has been studied by Ozdemir et al. [15]. In particular, they have found that LBO doped with CuO exhibits a single, well-

resolved and high-intensity TL peak at the low temperatures around 120°C. The TL properties of LBO doped with aluminium have been described in Ref. [16]. Following from the works mentioned above, one can conclude that Cu and Al are the most appropriate dopants for the LBO compounds.

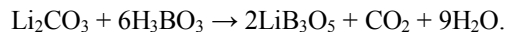
To obtain LBO, the authors of the works [11–16] have employed a solid-state synthesis typically performed at the temperatures lower than 1107 K (834°C). Such a condition impedes homogeneous distribution of a dopant within the sample volume. However, high abundance of B₂O₃ in LBO (3B₂O₃:1Li₂O) allows one to prepare easily the LBO glass by melting a batch, overheating it up to 1173 K (900°C) and then cooling it fast. Elevated temperature facilitates a homogeneous distribution of dopants in the glass, while fast cooling results in formation of crystallites. A crystallized glass (pyroceramic) with homogeneously distributed dopants can be prepared in this manner. Remarkably, the glass crystallized using this technique exhibits a substantially higher TL intensity if compared with that typical for the common LBO glass.

In the present study, we report on synthesis and studies of both undoped and Ag-doped lithium triborate pyroceramic. Basing on our earlier works [17–22] concerned with doped lithium-tetraborate single crystals, Li₂B₄O₇:Ag, we have chosen Ag as a promising sensitizer to improve the TL properties of LiB₃O₅ pyroceramic.

2. Material and methods

2.1. LBO glass preparation

Solid-state reaction was used for synthesizing the lithium-triborate compound. High-purity lithium carbonate Li₂CO₃ and boric acid H₃BO₃ were used as initial materials. The reagents were mixed in the proportion chosen according to the phase diagram of borate compounds [5]. AgNO₃ (0.1 mol. % of Ag) was added to a batch. The mixture was thoroughly ground in agate mortar to provide homogeneity. The batch was placed into a ceramic crucible. This was followed by slow heating up to the temperature 970 K (~ 700°C) in a resistive furnace, thus providing conditions for the chemical reaction



The LBO compound synthesized in this way was loaded into a Pt crucible and heated for 3–4 h up to the temperature 1170 K that exceeds the melting point. In order to get homogeneous distribution of the components, we kept the melt at that temperature during 1.0–1.5 h. Finally, the melt was spilled onto a clean flat metal substrate that was kept at ambient conditions.

2.2. Preparation of LBO pyroceramic samples

To determine the glass-transition temperature T_g for our samples, a differential thermal analysis was performed using a Paulik–Paulik–Erdey Q1500D derivatograph. The appropriate plot is shown in Fig. 1. The main features of the differential thermal curve for the LBO glass were treated using the notation of Ref. [23]. A broad dip in the DTA curve corresponds to the glass-transition temperature $T_g = 699$ K (426°C), whereas a sharp maximum is a manifestation of crystallization point $T_c = 862$ K (589°C) for the main composition of LBO glass. The next minima correspond to the melting point $T_m = 1032$ – 1066 K (759–793°C).

Glass samples were cut into pieces of desired dimensions (1 mm thick, with the

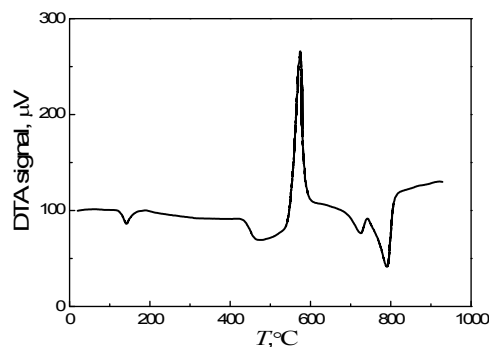


Fig. 1. DTA plot obtained for LiB₃O₅ glass.

approximate diameter of 5 mm), using a diamond saw. Then they were polished thoroughly. To prepare the LBO pyroceramic, the glass samples were subjected to heating treatment in a muffle furnace. The treatment was performed according to the following scenario. First, the samples were slowly heated up to the crystallization temperature $T_c = 862$ K during 4–5 h. After that they were kept at this temperature for 3 h and then slowly cooled down to the room temperature. Such a thermal processing results in formation of numerous microcrystals within the glass volume, so that the material reveals both crystalline and amorphous properties. Such a material is known as a glass-ceramics or pyroceramic.

2.3. Characterization of pyroceramic LBO sample

X-ray diffraction and SEM techniques were employed to characterize our LBO pyroceramic samples. The X-ray diffraction studies were performed with a standard diffractometer DRON-3 equipped with additional focusing system and a high-temperature chamber. A Bragg–Brentano geometry was used. Cu K_α radiation passed through a single graphite crystal that acted as a monochromator. Angular dependences of X-ray intensity were recorded with the accuracy 2% every 0.1° by a scintillation detector. An FEI Versa 3D scanning electron microscope with a resolution 0.8 nm was used for the SEM measurements. The SEM images observed for the LBO pyroceramic sample are shown in Fig. 2. One can clearly see LBO nanocrystals distributed randomly within the sample volume. The crystallites have an irregular rounded shape and the sizes of about 100–500 nm.

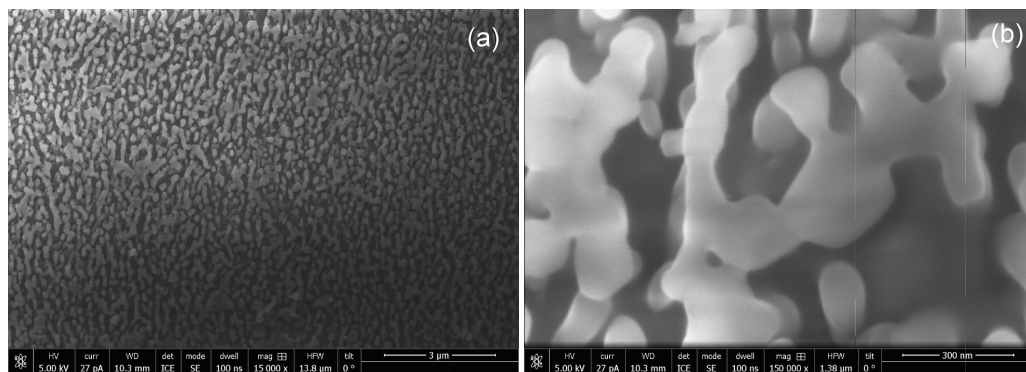


Fig. 2. SEM images obtained for our LBO pyroceramic at different magnifications: 15000 \times (a) and 150000 \times (b).

2.4. TL studies

Prior to the measurements of integrated TL parameters for the LBO pyroceramic, the samples were exposed to X-ray irradiation. A URC-55 device equipped with Mo anticathode operated at $U = 40$ kV and $I = 10$ mA was used as an X-ray source. The TL measurements were carried out separately inside two different temperature ranges, 80–325 and 293–540 K. In the former case, the sample was irradiated by X-quanta at 80 K. This was followed by heating with the rate 3.5 K/min. As for the second temperature range, the sample was exposed to X-ray irradiation at $T = 293$ K and the temperature increased with the rate 11.5 K/min. A photomultiplying tube FEP-39A was used to measure the TL radiation.

3. Results and discussion

Fig. 3 depicts the X-ray diffraction patterns observed for the polycrystalline (curve 1), pyroceramic (curve 2) and bulk-glass (curve 3) LBO samples. Sharp diffraction maxima seen on the curve 1

indicate a well-developed crystalline structure of polycrystalline LBO. On the contrary, a smooth diffraction pattern with broad peaks typical for curve 3 is a consequence of amorphous structure of the glass. It is worth noting that the diffraction pattern represented by curve 2 is intermediate.

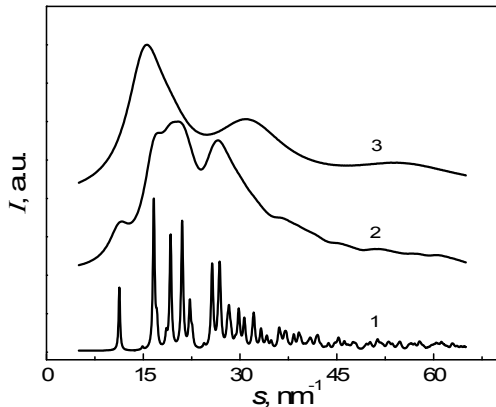


Fig. 3. X-ray diffraction patterns typical for different LBO samples: 1 – polycrystalline, 2 – pyroceramic, and 3 – bulk glass.

A simple comparison of the intensities corresponding to curves 2 and 3 and application of pair correlation function have indicated [24] that the local structures of pyroceramic and bulk-glass LBO compounds are quite similar. Even the shoulders observed on the l. h. s. of the principal peaks for the LBO pyroceramic correlate with the corresponding peaks for the bulk-glass sample. Therefore we conclude that the atomic distributions typical for both the pyroceramic and the glass demonstrate a high degree of short-range chemical ordering.

Fig. 4a depicts the integral TL curve obtained for the undoped LBO pyroceramic exposed to X-ray irradiation at 80 K. The integral TL plot contains two prominent maxima at the temperatures 123 and 269 K, as well as a number of weaker peaks located at 105, 142 and 169 K. The shape of the main TL peaks indicates that they arise from monomolecular recombination processes (the so-called first-order kinetics). The both peaks feature relatively slow ascent of their intensity if compared to a sharp decline.

The TL dependence reveals a different behaviour when the sample is irradiated at higher temperatures. One can clearly see from Fig. 4b that the integral TL curve for the undoped LBO pyroceramic exposed to X-ray irradiation at 293 K exhibits two broad main maxima centred at 376 and 413 K, as well as a weaker one located at 450 K. A two-fold increase in the X-ray irradiation dose results in some increase of the intensities of the main peaks, while the intensity of the peak at 450 K slightly decreases.

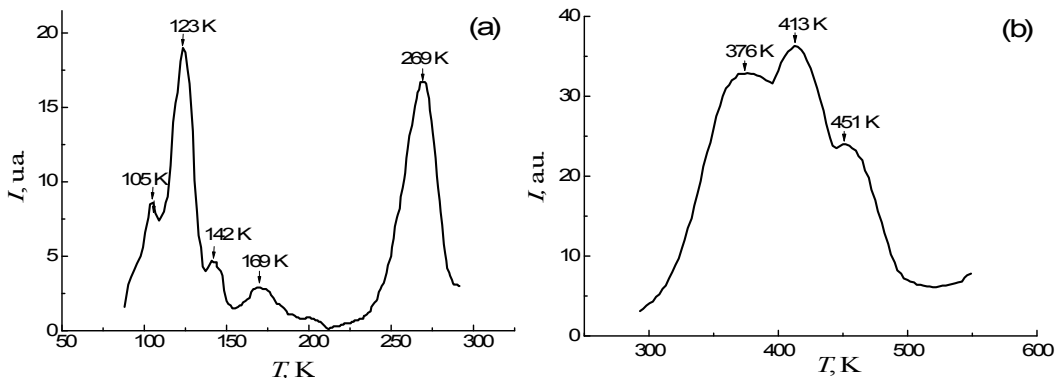


Fig. 4. Integral TL curves obtained for the LBO pyroceramic exposed to X-ray irradiation for 10 min: (a) $T = 80$ K, heating rate 3.5 K/min, and (b) $T = 293$ K, heating rate 11.5 K/min.

The activation energy E_a has been determined using a known Randall–Wilkins approximation that provides a simple formula $E_a = 25kT_m$ [25], where T_m is the temperature of the TL maximum and k the Boltzmann constant. The E_a values calculated for the undoped LBO pyroceramic are displayed in Table 1.

Table 1. Parameters T_m and E_a and intensity of the TL peaks obtained for undoped LBO pyroceramic (see the text).

| T_m , K | 105 | 123 | 142 | 169 | 269 | 376 | 413 | 450 |
|------------------|------|------|-----|------|------|------|------|------|
| E_a , eV | 0.22 | 0.26 | 0.3 | 0.36 | 0.57 | 0.78 | 0.89 | 0.97 |
| Intensity, a. u. | 8 | 19 | 4 | 2.5 | 14 | 33 | 37 | 25 |

I. N. Ogorodnikov et al. [26] have studied the TL for the undoped single LBO crystals in the temperature range 77–300 K. Basing on a detailed analysis of the photoluminescence and X-ray luminescence spectra, they have suggested that all of the TL peaks observed for the undoped single crystals in this temperature range can be attributed to localization of charge carriers on the electron (B^{2+}) and hole (O^-) traps. This happens during X-ray irradiation, followed by further delocalization upon heating. Remarkably, the TL spectra measured in the present work for the undoped LBO pyroceramic irradiated at 80 K coincide perfectly with those reported in Ref. [26]. Hence, one can explain the nature of the peaks at 105, 123, 142 and 169 K observed by us by the same processes. Indeed, the LBO pyroceramic contains nanocrystallites within the glass matrix (see Fig. 2), of which crystalline structure is the same as that observed for the single LBO crystals. Namely, the crystalline lattice of the LBO nanocrystallites can be viewed as a framework of anionic boron–oxygen complexes $[B_3O_7]^{5-}$, with Li^+ cations being surrounded by distorted oxygen tetrahedrons [27, 28].

However, the interpretation of the TL suggested in Ref. [26] for undoped LBO could not be applied to every TL peak observed by us in the temperature range 77–300 K. For instance, the TL peaks seen at $T_m = 240$ K and above 293 K can be associated with isovalent dopants that pollute the batch during the melt-solution synthesis. We make this conclusion basing on our complementary studies of the TL spectra for the LBO pyroceramic doped with Ag, which is isovalent to Li.

Fig. 5 depicts the integral TL curve for the LBO:Ag pyroceramic subjected to X-ray irradiation for 10 min. It is clearly seen that doping of the pyroceramic with Ag results in drastic changes of the integral TL signal when compared with that for the undoped pyroceramic (cf. the data of Fig. 4 and Fig. 5). The low-temperature peaks are much weaker than the intense peak observed at 282 K (see Fig. 5a). The TL intensity for the samples irradiated with X-rays at $T = 293$ K also exhibits substantial increase, with the maximum being centred at 406 K (see Fig. 5b).

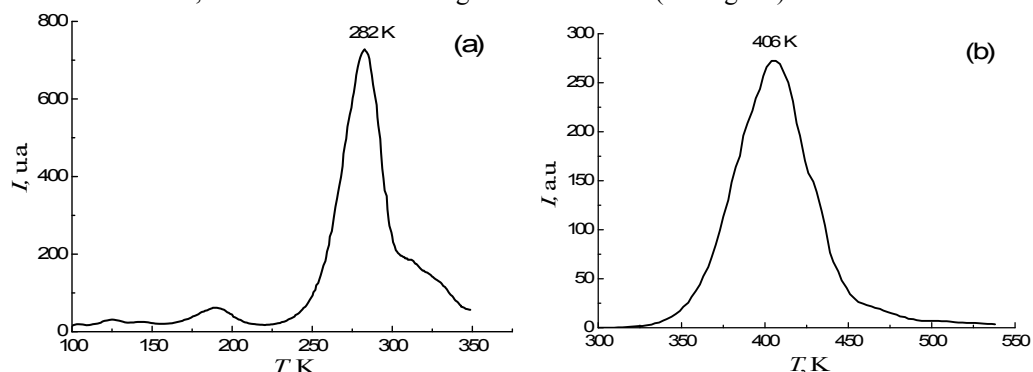


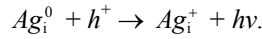
Fig. 5. Integral TL curves for LBO:Ag pyroceramic exposed to X-ray irradiation for 10 min: (a) $T = 80$ K, heating rate 3.5 K/min, and (b) $T = 293$ K, heating rate 11.5 K/min.

Apparently, the high-temperature TL peaks for the LBO:Ag pyroceramic are associated with Ag centres rather than boron–oxygen anion complexes. Therefore, the origin of those TL peaks needs to be explained by some processes other than those suggested in the work [26]. To find the appropriate explanation, we have used the results of our earlier studies on the TL properties of single $\text{Li}_2\text{B}_4\text{O}_7$:Ag crystals [18, 20, 21].

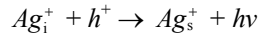
The crystalline lattice of the $\text{Li}_2\text{B}_4\text{O}_7$ single crystals can be represented as a framework comprised by boron–oxygen anion complexes $[\text{B}_4\text{O}_9]^{6-}$ with interplaced Li^+ cations surrounded by distorted oxygen tetrahedrons. The crystalline lattice of LBO appears to be very similar to that of the $\text{Li}_2\text{B}_4\text{O}_7$ single crystals. This allows one to assume the same TL nature for the $\text{Li}_2\text{B}_4\text{O}_7$ and LBO single crystals. The model of luminescent centres and the origin of TL in the single $\text{Li}_2\text{B}_4\text{O}_7$ crystals doped with Ag have been considered in our earlier studies [17–21]. We suggest that the non-irradiated LBO:Ag pyroceramic contains Ag^+ ions occupying both lithium sites Ag_s^+ and interstitial positions Ag_i^+ . X-ray irradiation of our doped pyroceramic results in formation of electron–hole pairs. The electrons trapped by Ag^+ ions at the lithium sites and the interstitial positions form Ag_i^0 atoms:



The holes are trapped next to the boron–oxygen anion complexes $[\text{B}_3\text{O}_7]^{5-}$. At first, heating activates the process



As a result, the TL peak appears near $T_m = 282$ K, with the activation energy 0.60 eV (see Fig. 4a). After heating is continued, the process



is activated. Then the TL peak appears near $T_m = 406$ K, with the activation energy 0.87 eV (see Fig. 4b).

Fig. 6 depicts the integral TL response for LBO:Ag observed at the temperature $T_m = 406$ K. As seen from Fig. 6a, all of the peaks exhibit a simple shape, with no prominent side peaks. The maximal intensity of the TL peak increases linearly with increasing X-ray irradiation dose (see Fig. 6b). This makes the TL properties of the LiB_3O_5 pyroceramic doped with Ag more favourable if compared to the pyroceramics with the other dopants. In particular, it is known that polycrystalline LBO doped with Al exhibits two peaks centred at 410 and 473 K, with different intensities. They reveal different responses to the same irradiation dose [15, 16]. Doping of LBO with Cu results in a single intense TL peak located at 393 K. However, as mentioned in Ref. [15], the behaviour of that peak is unstable, thus impeding applications of LBO:Cu in dosimetry.

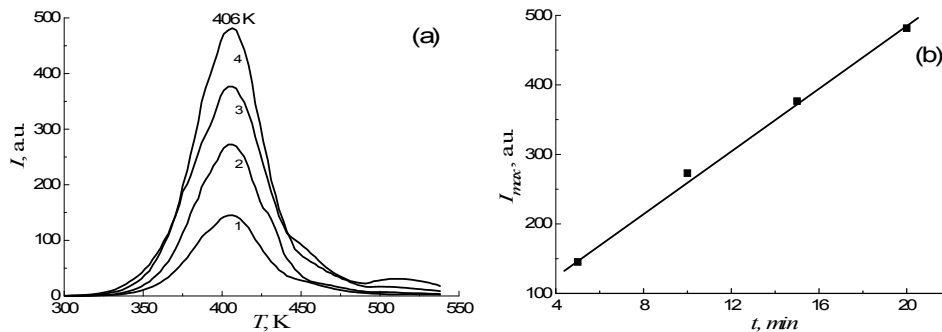


Fig. 6. (a) Dosimetric glow peaks observed for the LBO:Ag pyroceramic exposed to X-ray irradiation at $T = 293$ K: curves 1, 2, 3 and 4 correspond to the exposure times $t = 5, 10, 15$ and 20 min, respectively. (b) TL dose response determined by the peak height.

As a consequence, one can state that exceptional mechanical properties of the LBO:Ag pyroceramic, its low-cost preparation and a linear dependence of the TL response open wide prospects for that material in the field of radiation detecting. High abundance of ${}^6\text{Li}$ and ${}^{10}\text{B}$ isotopes also makes the LBO:Ag pyroceramic capable of neutron detection.

4. Conclusions

The LiB_3O_5 pyroceramic has been synthesized with the solid-state reaction technique. The formation of crystallites within the glass matrix has been achieved through melting and fast cooling of the glass, followed by annealing at the crystallization point. Both the undoped and Ag-doped LBO samples have been prepared. The X-ray diffraction studies and the scanning electron microscopy have confirmed formation of nanosized crystallites in the LiB_3O_5 glass.

The TL properties of the LBO pyroceramic have been studied. It has been found that the undoped pyroceramic exhibits a number of weak TL peaks in the temperature range of 80–500 K. They are associated with the luminescent centres in boron–oxide complex and with uncontrolled dopants. We have suggested the following model for the luminescent centres. Non-irradiated LBO:Ag pyroceramic contains both Ag^+ and Ag^{2+} ions. The Ag_s^+ ions occupy both the lithium sites Ag_s^+ and the interstitial positions Ag_i^+ . According to this model, the LBO:Ag pyroceramic exhibits two intense TL peaks located at 282 and 406 K after X-ray irradiation. We assign the peaks observed at 282 and 406 K to Ag_i^+ and Ag_s^+ ions, respectively. The TL peak seen at 406 K has a nearly perfect Gaussian shape. The TL dose response determined by the peak heights exhibits a linear dependence. This makes the LBO pyroceramic appealing for detecting any types of radiation. Due to the presence of ${}^6\text{Li}$ and ${}^{10}\text{B}$ isotopes, this also concerns the detection of neutrons. Our further studies will focus on improving the TL characteristics of the LBO:Ag pyroceramic. They will be aimed at the possible applications in personal dosimetry.

Acknowledgment

This work is partly supported by the Ministry of Education and Science of Ukraine under the Grants #0119U100357 and #0118U000267.

References

1. Driscoll M, Francis T and Richard J, 1984. The response of thermoluminescent materials to beta radiation. *Radiat. Prot. Dosimetry*. **9**: 295–298.
2. Fox P, Akber R and Pescott J, 1988. Spectral characteristics of six phosphors used in thermoluminescence dosimetry. *J. Phys. D*. **21**: 189–193.
3. Noh A, Amin Y, Mahat R and Bradley D, 2001. Investigation of some commercial TLD chips/discs as UV dosimeters. *Radiat. Phys. Chem.* **61**: 497–499.
4. Schulman J, Kirk R and West E. Use of lithium borate for thermoluminescence dosimetry. In: *Proc. USAEC Symp. Ser. 650637 (1967)*, p. 113.
5. Sastry B and Hummel F, 1958. Studies in lithium oxide systems: I, $\text{Li}_2\text{O B}_2\text{O}_3\text{--B}_2\text{O}_3$. *J. Amer. Ceram. Soc.* **41**: 7–17.
6. Beturne E and Touboul M, 1997. Synthesis of lithium borates ($\text{B/Li} \geq 3$) as LiB_3O_5 by dehydration of hydrated precursors. *J. Alloys Comp.* **255**: 91–97.
7. Moryc U and Ptak W, 1999. Infrared spectra of $\beta\text{-BaB}_2\text{O}_4$ and LiB_3O_5 : new nonlinear optical materials. *J. Mol. Struct.* **511**: 241–249.

-
8. Sabharwal S, Tiwari B and Sangeeta, 2003. Effect of highest temperature invoked on the crystallization of LiB_3O_5 from boron-rich solution. *J. Cryst. Growth.* **249**: 502–506.
 9. Ozdemir Z, Ozbaygly G, Kizilyalli M and Yilmaz A, 2004. Synthesis and characterization of lithium triborate. *Physicochem. Probl. Min. Proc.* **38**: 321–327.
 10. Depci T, Ozbaygly G and Yilmaz A, 2010. Comparison of different synthesis methods to produce lithium triborate and their effects on its thermoluminescent property. *Metall. Mater. Trans. A.* **41**: 2584–2594.
 11. Knitel M, Dorenbos P, van Eijk W, Plasteig B, Vianc B, Kahn-Harary A and Vivien D, 2000. Photoluminescence and scintillation/thermoluminescence yields of several Ce^{3+} and Eu^{2+} activated borates. *Nucl. Instr. Meth. A.* **443**: 364–374.
 12. El-Faramawy N, El-Kamesy S, El-Agramy A and Metwally G, 2000. The dosimetric properties of in-house prepared copper doped lithium borate examined using the TL-technique. *Radiat. Phys. Chem.* **58**: 9–13.
 13. M. Prokic, 2001. Lithium borate solid TL detectors. *Radiat. Meas.* **33**: 393–396.
 14. Depci T, Ozbaygly G and Yilmaz A, 2011. Synthesis and thermoluminescence properties of rare earth oxides (Y, Ce-Lu) doped lithium triborate. *J. Rare Earths.* **29**: 618–622.
 15. Ozdemir Z, Ozbaygly G and Yilmaz A, 2007. Investigation of thermoluminescence properties of metal oxide doped lithium triborate. *J. Mat. Sci.* **42**: 8501–8508.
 16. Kafadar V, Yazici A and Yildirim R, 2009. Determination of trapping parameters of dosimetric thermoluminescent glow peak of lithium triborate (LiB_3O_5) activated by aluminum. *J. Lumin.* **129**: 710–714.
 17. Adamiv V, Burak Ya, Girnyk I, Kasperchuk J, Kityk I and Teslyuk I, 1997. The growth and properties of K- and Ag-doped $\text{Li}_2\text{B}_4\text{O}_7$ single crystals. *Funct. Mater.* **4**: 415–418.
 18. Burak Ya, Adamiv V, Antonyak O, Malynych S, Pidzyrailo M and Teslyuk I, 2005. Thermoluminescence in doped single crystals $\text{Li}_2\text{B}_4\text{O}_7\text{:A}$ (A = Cu, Ag). *Ukr. J. Phys.* **50**: 1153–1158.
 19. Antonyak O, Adamiv V, Burak Ya and Teslyuk I, 2002. Thermoluminescence of doped $\text{Li}_2\text{B}_4\text{O}_7$ single crystals. *Funct. Mater.* **9**: 452–456.
 20. Adamiv V, Antonyak O, Burak Ya, Pidzyrailo M and Teslyuk I, 2005. Model of TSL-centers in $\text{Li}_2\text{B}_4\text{O}_7\text{:A}$ (A = Cu, Ag) single crystals. *Funct. Mater.* **12**: 278–281.
 21. Brant A, Kananan B, Murari M, McClory J, Petrosky J, Adamiv V, Burak Ya, Dowben P and Halliburton L, 2011. Electron and hole traps in Ag-doped lithium tetraborate ($\text{Li}_2\text{B}_4\text{O}_7$) crystals. *J. Appl. Phys.* **110**: 093719–7.
 22. Brant A, Buchanan D, McClory J, Adamiv V, Burak Ya, Halliburton L and Giles N, 2014. Photoluminescence from Ag^{2+} ions in lithium tetraborate ($\text{Li}_2\text{B}_4\text{O}_7$) crystals. *J. Lumin.* **153**: 79–84.
 23. Sontakke A, Biswas K, Tarafder A, Sen R and Annapurna A, 2011. Broadband Er^{3+} emission in highly nonlinear bismuth modified zinc-borate glasses. *Opt. Mater. Express.* **1**: 344–356.
 24. Padyak B, Mudry S, Kulyk Y, Drzewiecki A, Adamiv V, Burak Ya and Teslyuk I, 2012. Synthesis and X-ray structural investigation of undoped borate glasses. *Mater. Sci. (Poland)*. **30**: 264–273.
 25. Randall J and Wilkins M, 1945. Phosphorescence and electron traps. I. The study of trap distributions. *Proc. Roy. Soc. London, Ser. A.* **184**: 366–389.

-
26. Ogorodnikov I, Kruzhalov A, Radzhabov E and Isaenko L, 1999. Luminescent properties of crystalline lithium triborate LiB_3O_5 . Phys. Sol. State. **41**: 197–201.
27. Zachariasen W, 1964. The crystal structure of lithium metaborate. Acta Cryst. **17**: 749–751.
28. Burak Ya V, Moroz I Ye, 2003. Isostructural Phase transition in $\text{Li}_2\text{B}_4\text{O}_7$. Physics and Chemistry of Glasses. **44**: 241–243

Adamiv V. T., Burak Ya. V., Teslyuk I. M., Antonyak O. T., Moroz I. E. and Malynych S. Z. 2019. LiB_3O_5 pyroceramic for thermoluminescent dosimeters. Ukr.J.Phys.Opt. **20**: 159 – 167. doi: 10.3116/16091833/20/4/159/2019

***Анотація.** Досліджено процедури приготування та термолюмінесцентні властивості пірокераміки триборату літію (LiB_3O_5), легованої Ag. Її виготовлено за технологією спеціального відпалу скла LiB_3O_5 . Рентгенівські дифракційні дослідження пірокераміки виявили факт формування в аморфній матриці значної кількості нанорозмірних кристалітів. Обговорено кристалічну структуру та природу термолюмінесценції в пірокераміці LiB_3O_5 . Продемонстровано, що вона є матеріалом, перспективним для радіаційної дозиметрії.*